индекс 3624

ЕРЕВАНСКИЙ ФИЗИЧЕСКИЙ ИНСТИТУТ

ЕФИ-728(43)-84

ЦЕНТРАЛЬНЫЙ НАУЧНО-ИССЛЕДОВАТЕЛЬСКИЙ ИНСТИТУТ ИНФОРМАЦИИ И ТЕХНИКО-ЭКОНОМИЧЕСКИХ ИССЛЕДОВАНИЙ ПО АТОМНОЙ НАУКЕ И ТЕХНИКЕ

YU.G.SHAKHNAZARYAN

TRANSVERSE MOMENTUM DISTRIBUTION OF THE THREE-JET EVENT CROSS SECTION IN e^+e^--ANNIHILATION

ЕРЕВАН-1984

ЕФИ-728(43)-84

Ю.Г.ШАХНАЗАРЯН

РАСПРЕДЕЛЕНИЕ ПО ПОПЕРЕЧНОМУ ИМПУЛЬСУ СЕЧЕНИЯ ТРЕХСТРУЙНОГО СОБЫТИЯ В e^+e^- -АННИГИЛЯЦИИ

В первом порядке КХД вычислено дифференциальное по переменным T (импульсу наиболее энергичного партона) и $x_\perp$ (поперечному относительно оси $\vec{T}$ импульсу каждого из двух остальных партонов) сечение трехструйного процесса $e^+e^- \to q\bar{q}g$.Найдено также проинтегрированное по всем T в области допустимых для трехструйного события значений $2/3 \leqslant T \leqslant T_0$ распределение по поперечному импульсу. С целью выяснения возможности идентификации кварк-антикварковых и глюонных струй исследован вклад трех областей, различающихся относительной величиной импульса глюона, в полученные распределения.

Ереванский физический институт
Ереван 1984

The transverse momentum [1] is one of the parameters which allow to describe the observed in the e^+e^--annihilation three-jet events determined by the process

$$e^+ + e^- \to q + \bar{q} + g. \qquad (1)$$

Being the linear sum of transverse with respect to the single axis momenta of individual particles forming jets, this parameter, like the quantity T [2,3] , is less sensitive to the fragmentation mechanism of partons produced in the reaction (1) and allows to compare the experimental results with QCD predictions for the initial process (1). It has an obvious physical meaning - it is the transverse with respect to the $\vec{T}$ axis, the most energetic jet momentum, momentum of each of the two remaining jets in the reaction (1). The transverse momentum is an important characteristics of the three-jet event allowing to differ these events from two-jet ones, for which it is zero. This quantity along with T may be used as independent variables for the description of the process (1). Its square differs from the parameter S [4] by a constant factor only. The process (1) cross section, differential with respect to the variables T and S, is contained in ref. [3]*.

If we are interested in true three-jet events, we should exclude the regions corresponding to the emission of soft gluons and gluons escaping at the directions of quark and antiquark momenta from the phase volume permitted by the process (1) kinematics. In both cases we deal virtually with two-jet events. To exclude the latter, a cut-off parameter $T_0 < 1$ is introduced and as an admissible range of variation of T for the three-jet event the region $2/3 \leq T \leq T_0$ is considered [1].

In the present paper for three-jet events we have obtained a transverse momentum distribution at fixed value of T as well as a distribution integrated over all admissible values of T and have found the contribution of separate kinematic regions [5], that differ by the relative value of the gluon momentum, into the above distributions.

We shall proceed from the process (1) differential cross section integrated over angles which at energies, when the mass of quarks may be ignored, has the form [6,7]

$$\frac{d\sigma}{dx_1 dx_2} = \frac{8\alpha^2\alpha_s}{3S} \sum_a Q_a^2 \frac{x_1^2 + x_2^2}{(1-x_1)(1-x_2)}, \qquad (2)$$

where summation is carried out over all flavors, Q_a is the charge of the flavor a quark in the units e, α_s is the travelling coupling constant in QCD, S is the reaction total energy square, $\vec{x}_i = 2\vec{P}_i/\sqrt{S}$ is the dimensionless momentum of i-parton (i = 1,2,3 for $q, \bar{q}, g$ respectively).

Let us introduce the indices $i \neq j \neq k$ each taking the values 1,2,3, and assume that $x_i \geq x_j \geq x_k$, i.e. consider x_i to

* Note that the last two summands of the expression (2.8) given in the mentioned paper are incorrect.

be a dimensionless momentum of the most energetic parton ($x_i = T$) among the quark, antiquark and gluon produced in the reaction (1), and x_k to be the momentum of the least energetic parton. Let us now define the momentum transverse with respect to the axis $\vec{x}_i = \vec{T}$ (fig.1):

$$x_\perp^i = x_j \sin\theta_{ij} = x_k \sin\theta_{ik} \qquad (3)$$

Making use of the conservation laws of energy and momentum

$$x_i + x_j + x_k = 2, \quad \vec{x}_i + \vec{x}_j + \vec{x}_k = 0 \qquad (4)$$

we obtain

$$(x_\perp^i)^2 = 4\,\frac{(1-x_i)(1-x_j)(1-x_k)}{x_i^2}, \qquad (5)$$

whence, at the fixed value of $x_i = T$ we find limits of the variation of $x_\perp^2$:

$$4\,\frac{(1-T)^2(2T-1)}{T^2} \leq x_\perp^2 \leq 1-T. \qquad (6)$$

The phase volume in the variables T and $x_\perp$ is presented in fig.2. Absolute limits of variation of these variables correspond to points of intersection of curves $x_\perp = 2(1-T)(2T-1)^{1/2}/T$ and $x_\perp = (1-T)^{1/2}$: $x_\perp = 0$ at $T=1$, $x_\perp = 1/\sqrt{3}$ at $T=2/3$. At the fixed value of $x_\perp$ the $T_{max} = 1 - x_\perp^2$ corresponds to the kinematic configuration when $x_j = x_k$, and T_{min} is the root of equation $T_{min}^2 x_\perp^2 = 4(1-T_{min})^2(2T_{min}-1)$ and is realized in the case $x_i = x_j = T_{min}$.

In order to pass in the cross section (2) from the variables x_1 and x_2 that characterize quark and antiquark to the variables T and $x_\perp$, let us divide the phase volume into the regions:

$$\text{I)}\ x_1 \geq x_2 \geq x_3, \quad \text{II)}\ x_1 \geq x_3 \geq x_2, \quad \text{III)}\ x_3 \geq x_1 \geq x_2, \qquad (7)$$

i.e. we differentiate partons by their energies. We have not considered here the regions that are obtained from the given ones by means of replacements $x_1 \rightleftarrows x_2$, since due to the initial cross section (2) symmetry with respect to these replacements they give the same contribution in the cross section as the regions (7).

Using (4) and (5), let us express x_j and x_K via new independent variables $x_i = T$ and $x_\perp$:

$$x_j = 1 - \frac{T}{2}(1-y) \equiv x_+ , \quad x_K = 1 - \frac{T}{2}(1+y) \equiv x_- , \quad y \equiv \left(1 - \frac{x_\perp^2}{1-T}\right)^{1/2} . \quad (8)$$

Noting also that

$$dx_1 dx_2 = dx_i dx_j = \frac{T x_\perp}{2(1-T)y} dT dx_\perp$$

and normalizing the expression obtained from (2) to the total cross section of the e^+e^--annihilation to hadrons, which in the first approximation in α_s has the form

$$\sigma_{tot} \equiv \sigma(e^+e^- \to hadrons) = \frac{4\pi\alpha^2}{s}\left(1+\frac{\alpha_s}{\pi}\right)\sum_a Q_a^2 , \quad (9)$$

we may write down the differential cross section of interest for each of regions $n = I, II, III$ as follows:

$$\frac{1}{\sigma_{tot}} \frac{d\sigma_n}{dT dx_\perp} = \frac{2}{3} \frac{\alpha_s}{\pi} \left(1+\frac{\alpha_s}{\pi}\right)^{-1} \frac{T x_\perp}{(1-T)y} F_n , \quad (10)$$

where $F_n = (x_1^2 + x_2^2)/(1-x_1)(1-x_2)$ is the function that distinguishes these regions. In virtue of the fact that the quark and antiquark jets are topologically indistinguishable, a factor 2, that allows also for the contribution of the above regions, is added to the right hand part of the expression (10).

In the region I, where the gluon jet is the least energetic, one should put $i = 1$, $j = 2$, $K = 3$. Then

$$F_I = \frac{T^2 + x_+^2}{(1-T)(1-x_+)} . \quad (11)$$

In the region II, where the gluon jet is intermediate in energy ($i = 1$, $j = 3$, $K = 2$), we have

$$F_{II} = \frac{T^2 + x_-^2}{(1-T)(1-x_-)} . \quad (12)$$

And, finally, in the region III, where the gluon jet is the most energetic ($i = 3$, $j = 1$, $K = 2$), we obtain

$$F_{III} = \frac{x_+^2 + x_-^2}{(1-x_+)(1-x_-)} . \quad (13)$$

If we are not interested in the origin of jets, i.e. the fact whether this or that jet produced in the reaction (1), due to fragmentation of quark (antiquark) or gluon , the total distribution in T and $x_\perp$ will have the form

$$\frac{1}{\sigma_{tot}} \frac{d\sigma}{dT dx_\perp} = \frac{2}{3} \frac{\alpha_s}{\pi} \left(1+\frac{\alpha_s}{\pi}\right)^{-1} \frac{T x_\perp}{(1-T)y} \left[\frac{T^2+x_+^2}{(1-T)(1-x_+)} + \frac{T^2+x_-^2}{(1-T)(1-x_-)} + \frac{x_+^2+x_-^2}{(1-x_+)(1-x_-)}\right] (14)$$

The integration of this expression over the transverse momentum within the limits of (6) leads to the result obtained for $d\sigma/dT$ in [3].

Note that the quantity defined as follows

$$\left(1+\frac{\pi}{\alpha_s}\right) \frac{1}{\sigma_{tot}} \frac{d\sigma_n}{dT dx_\perp} = \frac{2}{3} \frac{T x_\perp}{(1-T)y} F_n$$

where F_n is given by one of expressions (11)-(13) as well as the relevant total distribution are functions of dimensionless variables T and $x_\perp$ only and should have the same dependence on these variables independent of the reaction energy. Only the cut-off parameter T_0 introduced to exclude the two-jet events (see below) may be energy-dependent, and even then, apparently, weakly.

To obtain quantitative representation on the contribution of each region (7) into the total distribution, we have shown in fig.3 the dependence of the quantity

$$\left(1+\frac{\pi}{\alpha_s}\right)\frac{1}{\sigma_{tot}}\frac{d\sigma_n}{dx_\perp dy}=\frac{4}{3}\frac{T(1-T)}{x_\perp}F_n \quad (n=\mathrm{I},\mathrm{II},\mathrm{III}) \qquad (15)$$

on the transverse momentum as well as the total distribution at some values of the parameter T. Limits of variation of the transverse momentum (with an accuracy of parts per thousand) are plotted in the table at each considered value of T. With the increase in T in the range $2/3 < T < T_0$ the region of admissible values of $x_\perp$ grows (fig.2). For the cut-off parameter T_0 here and further the value $T_0 = 0.95$ is taken.

Let us explain the curves depicted in fig.3 after the example of $T = 0.95$. In the region I the cross section (15) falls with the increase in the transverse momentum from the minimum value of $x_\perp$ at the given T to the maximum (these values are shown by vertical dotted line). In the region II with the increase in the transverse momentum the cross section first decreases then increases (at $T \leq 0.80$ only increase is observed). Finally, in the region III the cross section falls with the increase in $x_\perp$. At $x_\perp = x_{\perp min}(T)$ the cross sections in the regions II and III are numerically equal. This is due to the fact that at the given T the minimum value of the transverse momentum is realized in the case $x_i = x_j = T$ when, in accord with (8), $x_+ = T$ and the expressions (12) and (13) coincide. The equality of cross sections in the regions I and II at $x_\perp = x_{\perp max}(T)$ follows from the fact that at $x_j = x_K$ which is the case here, $x_+ = x_-$ and $F_I = F_{II}$. It is clear from the physical point of view that on the boundaries of regions the conversion from one region to another takes place.

Consider now the contribution of separate regions into the total distribution which is represented by the upper curve at

the corresponding value of T. The relative portion (on a percentage basis) of the cross section (15) for separate regions in the total cross section is plotted in the table for minimum and maximum values of the transverse momentum at the given T. Note that with the variation of the transverse momentum, relative contributions of the regions considered smoothly vary within the limits shown in the table. Note first of all that as distinct from the other two regions, the relative contribution of the region III does not practically vary with the transverse momentum at all values of T (the instability makes less than a per cent). This comes through in the fact that in fig.3 the total distribution at every T exactly repeats the behavior with the variation of $x_\perp$ of the cross section (15) in the region III.

At small values of T, e.g. $T = 0.7$, there is no noticeable domination of any region. Therefore, in this case the total distribution curve lies considerably higher than its components. With the increase in T the contribution of the region III decreases and that of the region I increases at all admissible values of $x_\perp$, whereas the contribution of the region II near the lower limit of the $x_\perp$ variation decreases and near the upper limit increases. As a result, at large T near the upper limit of the $x_\perp$ variation the basic contribution into the total distribution is made by the regions I and II, and near the lower limit by the region I. So one may state that at $T = 0.90$ in 94 cases out of 100 the jet with the maximum momentum is a quark-antiquark one at all admissible values of $x_\perp$, and on the lower limit of $x_\perp$ the jet with the minimum momentum is gluonic in 88 cases out of 100. At $T = 0.95$ the appropriate numbers are more favorable from the viewpoint of identification of quark-antiquark and gluon jets: in more than 97 % the jet with the maximum momentum is a quark-antiquark one, and in nearly 95 % of cases the jet with the minimum **momentum** is a gluon one (on the lower limit of $x_\perp$ variation).

In case we are interested in experiment in the events with a definite value of the transverse momentum $x_\perp$ independent of the value T, which will allow to have more statistics, the cross section may be obtained from (14) by integration over T :

$$\frac{d\sigma}{dx_\perp} = \int_{T_{min}}^{T_0} dT \frac{d\sigma}{dT dx_\perp}, \quad \frac{2(1-T_0)}{T_0}(2T_0-1)^{1/2} \leqslant x_\perp \leqslant (1-T_0)^{1/2}, \qquad (16)$$

$$\frac{d\sigma}{dx_\perp} = \int_{T_{min}}^{1-x_\perp^2} dT \frac{d\sigma}{dT dx_\perp}, \quad (1-T_0)^{1/2} \leqslant x_\perp \leqslant 1/\sqrt{3},$$

where T_{min} is the root of the third power equation that is written out above.

At $T_0 = 0.95$ that we use for the cut-off parameter, the first integral is defined in the region $0.100 \leqslant x_\perp \leqslant 0.224$. One should bear in mind that at values of $x_\perp$ in the noted region, as follows from fig.2, there may be events with $T > T_0 = 0.95$, which however should not be considered if one wishes to restrict himself to three-jet events and the cut-off parameter T_0 is chosen correctly.

In fig.4 the dependence of $(1+\pi/\alpha_s)\sigma_{tot}^{-1}\, d\sigma/dx_\perp$ on the transverse momentum (upper curve) is presented as well as the contribution of separate regions (7) into the mentioned distribution. Fractures on the curves correspond to the matching point $x_\perp = (1-T_0)^{1/2} = 0.224$ of the integrals (16) (left branches are described by the first integral, and right ones by the second). At small values of the transverse momentum

($x_\perp \leqslant 0.16$) the basic contribution into the dependence considered is made by the region I (more han 90%), and the contribution of the regions II and III is small and nearly equal. With the increase in $x_\perp$ the relative contribution of the region I decreases and that of regions II and III increases. Near the upper limit of $x_\perp$ contributions of all regions become equal.

The choice of the parameter T_0 determines the lower limit of variation of $x_\perp$ and, hence, the arrangement of left branches of distribution curves depicted in fig.4. With the increase in T_0 the region of admissible $x_\perp$ will begin from lower values, and fractures on curves will shift to the left. It is unlikely that experimental data will allow to find a fracture on the distribution curve (upper curve in fig.4). Most likely a smooth transition will be observed between its left and right branches. However, one may judge of the value of T_0 by the arrangement of the part where the fall of the curve begins (left branch).

Table

T	$x_\perp$ extremum	Relative contribution of separate regions in the total distribution (in %)		
		n = I	n = II	n = III
0.70	0.542	43.46	28.27	28.27
	0.548	35.79	35.79	28.42
0.75	0.471	58.06	20.97	20.97
	0.500	39.27	39.27	21.46
0.80	0.387	70.58	14.71	14.71
	0.447	42.37	42.37	15.26
0.85	0.295	80.58	9.71	9.71
	0.387	45.01	45.01	9.98
0.90	0.199	88.40	5.80	5.80
	0.316	47.15	47.15	5.70
0.95	0.100	94.68	2.66	2.66
	0.224	48.80	48.80	2.40

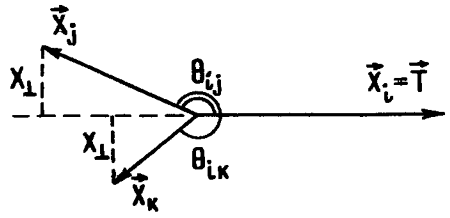

Fig.1.

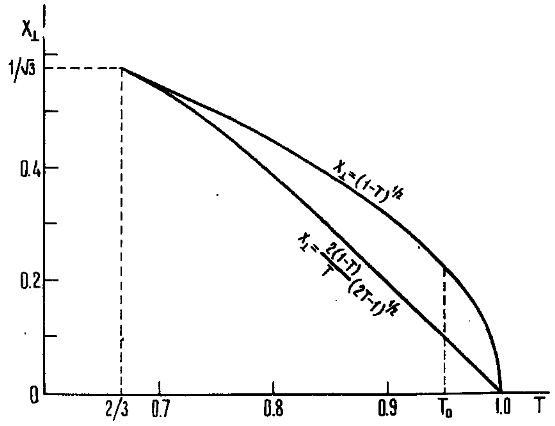

Fig.2

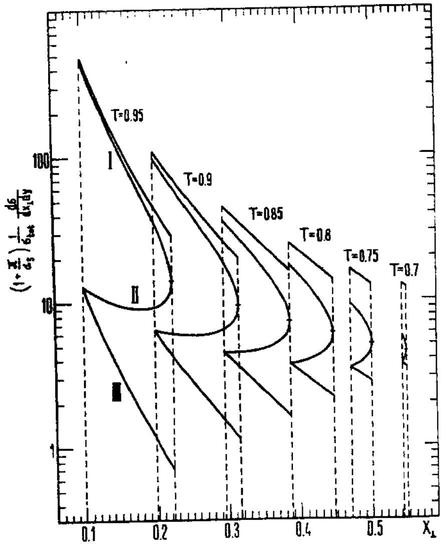

Fig 3

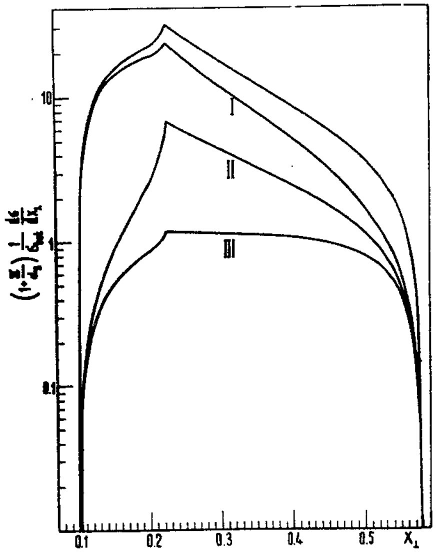

Fig.4

Figure Captions

Fig.1. Three-jet event kinematics.

Fig.2. Phase volume of the process (1) in variables T and $x_\perp$.

Fig.3. Double differential cross section of the process (1) as a function of the transverse momentum at some values of the parameter T (upper curves). Contributions of separate regions (7) are depicted by appropriate parts of curves between dotted lines (for the value $T = 0.95$ they are denoted by I,II and III).

Fig.4. Distribution in the transverse momentum of the process (1) cross section (upper curve) and contribution of separate regions (7) into the mentioned distributior (appropriate curves are denoted by I,II and III).

References

1. Hoyer P., Osland P., Sander H.G. et al. Quantum Chromodynamics and Jets in e^+e^-. - Nucl.Phys.,1979,vol.B161,p.349.
2. Farhi E. Quantum Chromodynamics Test for Jets. - Phys.Rev. Lett.,1977,vol.39,p.1587.
3. De Rujula A., Ellis J., Floratos E.G., Gaillard M.K. QCD Predictions for Hadronic Final States in e^+e^- Annihilation.- Nucl.Phys.,1978,vol.B138,p.387.
4. Georgi H., Machacek M. Simple Quantum-Chromodynamics Prediction of Jet Structure in e^+e^- Annihilation. - Phys.Rev. Lett.,1977,vol.39,p.1237.
5. Шахназарян Ю.Г. Распределение по T трехструйных событий в e^+e^--аннигиляции для тяжелых кварков. - ЯФ, 1982, т.35, с.438.
6. Ellis J., Gaillard M.K., Ross G.G. Search for Gluons in e^+e^- Annihilation. - Nucl.Phys.,1976,vol.B111,p.253; Erratum,ibid,1977,vol.B130,p.516.
7. De Grand T.A., Ng Y.J., Tye S.-H.H. Jet Structure in e^+e^- Annihilation as a Test of Quantum Chromodynamics and the Quark-confining String. - Phys.Rev.,1977,vol.D16,p.3251.

The manuscript was received 14 May 1984

ШАХНАЗАРЯН Ю.Г.

РАСПРЕДЕЛЕНИЕ ПО ПОПЕРЕЧНОМУ ИМПУЛЬСУ СЕЧЕНИЯ ТРЕХСТРУЙНОГО СОБЫТИЯ В e^+e^- -АННИГИЛЯЦИИ

(на аглийском языке, перевод Л.Н.Багдасаряна)

Редактор Л.П.Мукаян
Технический редактор А.С.Абрамян

Подписано в печать 25/XII-84г. ВФ-03032 Формат 60x84/16
Офсетная печать.Уч.изд.л.1,0 Тираж 299 экз.Ц. 15 к.
Зак. тип. № 947 Индекс 3624

Отпечатано в Ереванском физическом институте
Ереван 36, Маркаряна 2